Stimuli responsive smart-gels realized via modular protein design

Tijana Z. Grove[1], **Chinedum O. Osuji**[2], **Jason D. Forster**[3], **Eric R. Dufresne**[2,3,4,5], and **Lynne Regan**[1,6,*]

[1]Molecular Biophysics and Biochemistry, Yale University, New Haven, 06511, USA

[2]Chemical and Environmental Engineering, Yale University, New Haven, 06511, USA

[3]Mechanical Engineering and Materials Science, Yale University, New Haven, 06511, USA

[4]Physics, Yale University, New Haven, 06511, USA

[5]Cell Biology, Yale University, New Haven, 06511, USA

[6]Department of Chemistry, Yale University, New Haven, 06511, USA

Abstract

Smart-gels have a variety of applications including tissue engineering and controlled drug delivery. Here we present a modular, bottom-up approach that permits the creation of protein-based smart-gels with **encoded** morphology, functionality, and responsiveness to external stimuli. The properties of these gels are encoded by the proteins from which they are synthesized. In particular, the strength and density of the network of intermolecular cross-links are specified by the interactions of the gel's constituent protein modules with their cognate peptide ligands. Thus, these gels exhibit stimuli-responsive assembly and disassembly, dissolving (or gelling) under conditions that weaken (or strengthen) the protein-peptide interaction. We further demonstrate that such gels can encapsulate and release both proteins and small molecules and that their rheological properties are well suited for biomedical applications.

Harnessing proteins to create smart-gels with an array of applications, including tissue regeneration scaffolds and controlled drug delivery devices, has been much anticipated[1–10]. The gel designs we present are based on the 34 amino acid tetratricopeptide repeat (TPR)[11]. The modular construction of repeat proteins allows many different permutations and combinations of their constituent modules to be rapidly created and tested. Moreover, additional modules can be readily incorporated to introduce additional functions, such as cell-specific binding. Natural TPR domains facilitate the assembly of macromolecular complexes, held together by specific TPR-peptide interactions[12].

The TPR adopts a helix-turn-helix structure, which in tandem arrays forms a rigid superhelix with eight repeats per superhelical turn (Fig.1 A–B). The properties of individual TPR units can be manipulated, and the stability of arrays of TPRs can be predicted, based on their constituent units[13–16]. TPR modules can be engineered to bind different peptide ligands: Such binding is highly specific and a variety of TPR modules with different binding specificities and affinities have been created in our laboratory[17–22]. Individual TPR units can thus be mixed and matched in a modular fashion to create proteins of predictable structure,

stability and function. Consequently, TPR arrays show tremendous promise for the assembly of biomaterials with an unprecedented degree of tunability. Moreover, the TPR-peptide interaction is robust in the presence of non-specific proteins; for example mock serum 7%BSA (Kevin Lai, Robert Collins, TZG, LR, unpublished data).

In our strategy, TPR arrays are cross-linked by multi-valent peptide ligands[23,24] to create percolating three-dimensional networks (Fig.1C). Specifically, the TPR protein incorporates both peptide-binding and "spacer" 3TPR modules, arrayed along the superhelix such that the cross-linking is specific, directional, and inter-protein cross-links are favored (Fig 1B). Upon mixing the TPR array and the PEG-peptide component, self-supporting hydrogels form spontaneously at room temperature (Fig 2A). Gelation does not require chemical cross-linking reagents, redox chemistry, or extreme conditions, all of which could preclude *in vivo* applications[6,10].

Here, we present the characterization of gels formed from 1% weight per volume TPR in aqueous solution, with a 1:2 ratio of TPR peptide binding sites to peptide units (Fig 2). The resultant gels are cross-linked by specific non-covalent interactions between binding modules of the repeat protein and their peptide ligands. Because such interactions are intrinsically reversible, gelation is also reversible under conditions determined by the nature of protein-peptide interaction. The kinetics of gel formation depend on the concentration of the components, the ratio of TPR peptide-binding domains to peptides, and solution conditions. Detailed phase diagrams and kinetic studies of gelation will be presented elsewhere.

We characterized the viscoelastic properties of the gels using both micro and bulk rheology. In microrheology measurements, we tracked the Brownian motion of 100 nm radius fluorescent probe particles[25]. The TPR or peptide solutions alone (or the mixture immediately post-mixing) display liquid-like behavior, with the probe particles moving freely (Fig. 2B). By contrast, after gelation, the probe particles become trapped in the gel, and their mean-square displacement is independent of time across the range of timescales observed. Thus, the material entraps the probe particles, and is actually too strong for us to accurately estimate the storage and loss moduli in this experimental set-up. In bulk rheology measurements[26], gelation is evidenced by the emergence of a frequency independent elastic modulus (G') (Fig. 2C). Initially, the mixture of the TPR and peptide components exhibits liquid-like behavior, with an elastic modulus too small to be effectively measured ($<\sim 5$Pa). Upon gelation, the elastic modulus increases to 270 Pa, comparable to the elastic modulus of a gel made of 15% Jell-O, or 5% polyacrylamide/bisacrylamide[27]. An elastic modulus of 270 Pa is more than sufficient to maintain mammalian cells in suspension for tissue regeneration applications, the minimum requirement for which has been estimated as 50 to 100 Pa[9,28].

The gel exhibits a remarkably large linear viscoelastic regime and can be stretched 10 times its thickness before it yields. Upon relaxation it recovers its elasticity and can be stretched and relaxed repeatedly (Fig 2D). Such high yield-strains are unprecedented for non-covalently cross-linked polymer and biopolymer gels. Interestingly, the gel displays a modest strain stiffening in advance of yielding, likely due **to** the finite extensibility of the PEG-peptide crosslinker. While it is generally not observed in synthetic polymer gels, strain stiffening is a near ubiquitous feature in the rheology of many biological materials, where it aids in the prevention of excessive deformations[29]. The rheological properties that our gels exhibit are well-suited for biological applications which require soft yet elastic media with good mechanical integrity[30].

There are many ways in which to incorporate stimuli responsiveness into TPR-based gels. The gel design we present here is cross-linked by the specific non-covalent interaction of the peptide DESVD-COO$^-$ with a specific TPR binding unit. This interaction is predominantly electrostatic and thus its strength decreases as the ionic strength increases. Specifically, in 10 mM NaCl the dissociation constant of the peptide-TPR interaction is 5 µM and this value decreases to 300 µM when the salt concentration is increased to 500 mM.. Therefore these gels erode in high salt. Fig. 3a shows the time-course of erosion of gels placed in solutions of different ionic strength. The higher the concentration of salt, the faster the gel dissolves. This process is reversible – when the salt concentration is decreased, the gel reforms.

A desirable property of smart materials, related to their potential application in drug delivery, is the ability to encapsulate and subsequently release entrapped materials. To test the ability of these smart-gels to sequester and release content, we included a fluorescent protein, mVFP (26 kDa), in the gelation mixture[31]. The resulting gels fully encapsulate the protein in a functional state, indicated by its fluorescence. The gels show negligible leakage of the protein when immersed for weeks in a solution of low ionic strength. When placed in a solution of higher ionic strength, however, the fluorescent protein is released and the kinetics of release directly mirrors the kinetics of gel erosion (Fig. 3B). Such deliberate, stimuli-responsive release is well suited to possible application of these materials as protein or nucleic acid delivery devices.

We also studied the entrapment and release of small 'drug mimetic' molecules by these gels. We encapsulated the fluorescent molecule, rhodamine (MW 422 Da), by including it in the gelation mix. The release of rhodamine is more rapid than the release of mVFP, but is also facilitated by increasing the ionic strength of the solution. However, in this case release precedes gel erosion (Figure 3C). The difference in release behaviour for mVFP and rhodamine is most simply rationalized by the relative sizes of these molecules; however, the interactions between TPR and mVFP proteins may also play a role.

In summary, we have fabricated ionic-strength responsive hydrogels by using modular bottom up protein design. These gels are cross-linked by specific, non-covalent interactions between repeat protein modules and their partner peptide ligands. The ability of the gels to encapsulate and release both large and small molecules bodes well for their potential use in controlled drug delivery applications. The robust elastic modulus and extraordinary elasticity of these gels suggests that with application-specific optimization, these gels will be well suited for cell culture and tissue engineering applications. Although we have presented the characterization of just one example of this type of smartgel design, the combination of modular TPR structure, specific and predictable self-assembly, and versatility of functionalization makes this approach a compelling path towards realizing new multifunctional materials with an array of tunable properties.

Supplementary Material

Refer to Web version on PubMed Central for supplementary material.

Acknowledgments

References

1. Banwell EF, Abelardo ES, Adams DJ, Birchall MA, Corrigan A, Donald AM, Kirkland M, Serpell LC, Butler MF, Woolfson DN. Nat Mater. 2009; 8:596–600. [PubMed: 19543314]

2. Jia X, Kiick KL. Macromol Biosci. 2009; 9:140–156. [PubMed: 19107720]

3. Maskarinec SA, Tirrell DA. Curr Opin Biotechnol. 2005; 16:422–426. [PubMed: 16006115]

4. Petka WA, Harden JL, McGrath KP, Wirtz D, Tirrell DA. Science. 1998; 281:389–392. [PubMed: 9665877]

5. Rajagopal K, Lamm MS, Haines-Butterick LA, Pochan DJ, Schneider JP. Biomacromolecules. 2009; 10:2619–2625. [PubMed: 19663418]

6. Sengupta D, Heilshorn SC. Tissue Eng Part B Rev. 2010; 16:285–293. [PubMed: 20141386]

7. Shen W, Zhang K, Kornfield JA, Tirrell DA. Nat Mater. 2006; 5:153–158. [PubMed: 16444261]

8. Topp S, Prasad V, Cianci GC, Weeks ER, Gallivan JP. J Am Chem Soc. 2006; 128:13994–13995. [PubMed: 17061859]

9. Wong Po Foo CT, Lee JS, Mulyasasmita W, Parisi-Amon A, Heilshorn SC. Proc Natl Acad Sci U S A. 2009; 106:22067–22072. [PubMed: 20007785]

10. Branco MC, Schneider JP. Acta Biomater. 2009; 5:817–831. [PubMed: 19010748]

11. D'Andrea L, Regan L. Trends Biochem. Sci. 2003; 28:655–662. [PubMed: 14659697]

12. Scheufler C, Brinker A, Bourenkov G, Pegoraro S, Moroder L, Bartunik H, Hartl FU, Moarefi I. Cell. 2000; 101:199–210. [PubMed: 10786835]

13. Cortajarena AL, Lois G, Sherman E, O'Hern CS, Regan L, Haran G. J Mol Biol. 2008; 382:203–212. [PubMed: 18644382]

14. Cortajarena AL, Regan L. Protein Sci. 2006; 15:1193–1198. [PubMed: 16641492]

15. Kajander T, Cortajarena AL, Main ER, Mochrie SG, Regan L. J Am Chem Soc. 2005; 127:10188–10190. [PubMed: 16028928]

16. Kajander T, Cortajarena AL, Mochrie S, Regan L. Acta Crystallogr D Biol Crystallogr. 2007; 63:800–811. [PubMed: 17582171]

17. Cortajarena AL, Liu TY, Hochstrasser M, Regan L. ACS Chem Biol. 2010; 5:545–552. [PubMed: 20020775]

18. Cortajarena AL, Wang J, Regan L. Febs J. 2010; 277:1058–1066. [PubMed: 20089039]

19. Cortajarena AL, Yi F, Regan L. ACS Chemical Biology. 2008; 3:161–166. [PubMed: 18355005]

20. Grove TZ, Hands M, Regan L. Protein Eng Des Sel. 2010; 23:449–455. [PubMed: 20304973]

21. Jackrel ME, Cortajarena AL, Liu TY, Regan L. ACS Chem Biol. 2010; 5:553–562. [PubMed: 20038141]

22. Jackrel ME, Valverde R, Regan L. Protein Sci. 2009; 18:762–774. [PubMed: 19309728]

23. Lutolf MP, Hubbell JA. Biomacromolecules. 2003; 4:713–722. [PubMed: 12741789]

24. Yamaguchi N, Kiick KL. Biomacromolecules. 2005; 6:1921–1930. [PubMed: 16004429]

25. Dasgupta BR, Weitz DA. Phys Rev E Stat Nonlin Soft Matter Phys. 2005; 71:021504–021602. [PubMed: 15783330]

26. Yan C, Pochan DJ. Chem Soc Rev. 2010; 39:3528–3540. [PubMed: 20422104]

27. Fonkwe LG, Narsimhan G, Cha AS. Food Hydrocolloids. 2003; 17:871–883.

28. Kretsinger JK, Haines LA, Ozbas B, Pochan DJ, Schneider JP. Biomaterials. 2005; 26:5177–5186. [PubMed: 15792545]

29. Storm C, Pastore JJ, MacKintosh FC, Lubensky TC, Janmey PA. Nature. 2005; 435:191–194. [PubMed: 15889088]

30. Discher DE, Janmey P, Wang YL. Science. 2005; 310:1139–1143. [PubMed: 16293750]

31. Ilagan RP, Rhoades E, Gruber DF, Kao HT, Pieribone VA, Regan L. Febs J. 2010; 277:1967–1978. [PubMed: 20345907]
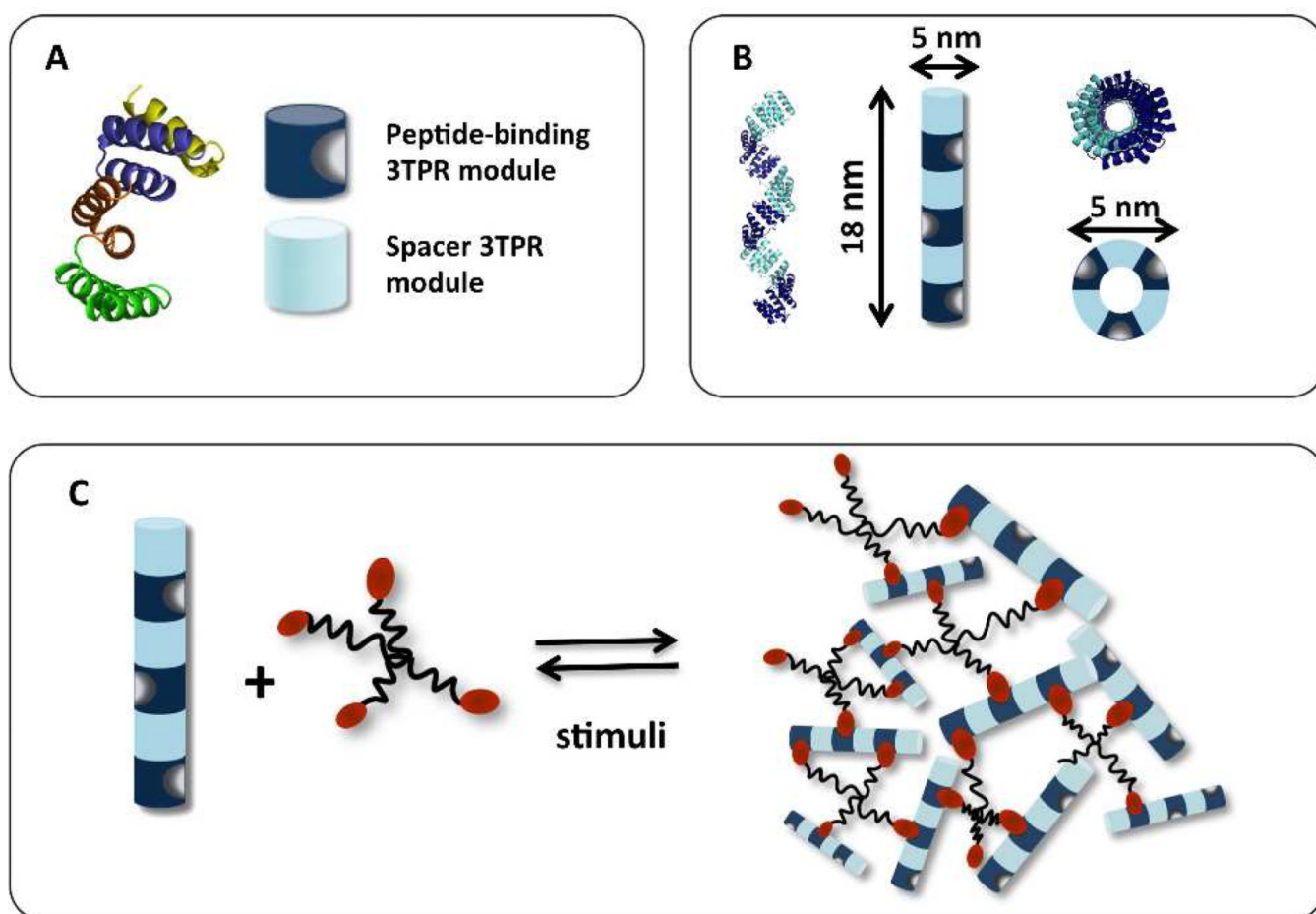
Figure 1. Modularity of TPR proteins allows the design of smartgels with predetermined structures

(A) Ribbon and cartoon representations of the structure of the 3TPR module used as either a spacer or a binding unit in the gel designs (based on PDB 1NA0). Each component 34 amino acid repeat is shown in a different color in the ribbon representation. The thermodynamic stability of both the spacer and binding modules can be varied greatly – from a melting temperature of less than 37° C to over 100° C[11,14]. The specificity and affinity of the binding module can also be manipulated. (b) Ribbon and cartoon representations of the structure of an 18TPR array, side and end on views (based on PDB 2FO7)[16]. The 3TPR modules are colored as in 1A. The superhelical rise is 1 nm per repeat, and 8TPR repeats form one turn of the superhelix: The 18TPR array is 18nm long with an outer diameter of 5nm. (C) Cartoon representation of TPR gel formation. The PEG-peptide cross-linker is represented by black lines for the PEG component and red ovals for the peptide. The cartoon is drawn approximately to scale – each arm of the 10kD four-arm star PEG has a contour length of ~ 18nm.
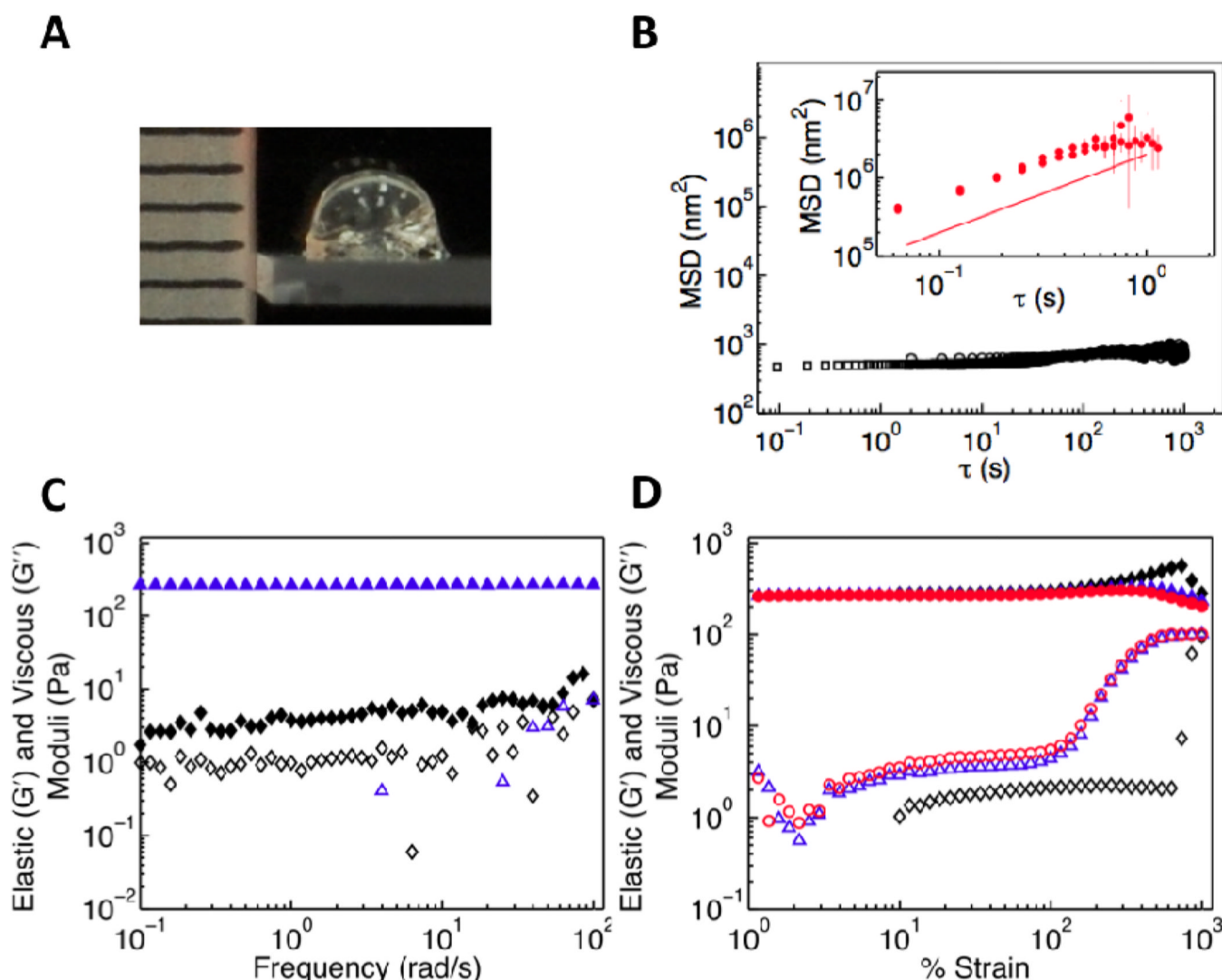
Figure 2. TPR-based smart-gels are self-supporting, soft yet elastic materials
(A) Photograph of a gel cast in the bottom of a microcentrifuge tube. A ruler is shown alongside for scale - 1 tick corresponds to 1mm. (B) Microrheology measurements tracking the Brownian motion of fluorescent probe particles. The mean square displacement is plotted as a function of time. The data for individual gel components is shown as red squares, with a line of slope = 1 drawn for comparison. The data for the gel, 21 days post mixing, is shown as open black squares. (C) Frequency dependence of the elastic modulus (G' – closed symbols) and the viscous modulus (G'' – open symbols). Behavior at the onset of gelation (diamonds, 243 h post-mixing) and close to the end of gelation (triangles, 292 h post-mixing) is shown. Defining characteristics of a gel are (i) the value of G' is independent of frequency and (ii) the value of G' is larger than G''. Both these conditions are clearly met by the TPR smart-gels. (D) Iterative strain sweeps, (black, blue, red in order of acquisition: Elastic modulus (G', solid diamonds) and viscous modulus (G'', open diamonds). The strain-hardening followed by yielding at 1000% strain is evident. The elastic modulus recovers to its initial value after repeated strain sweeps.
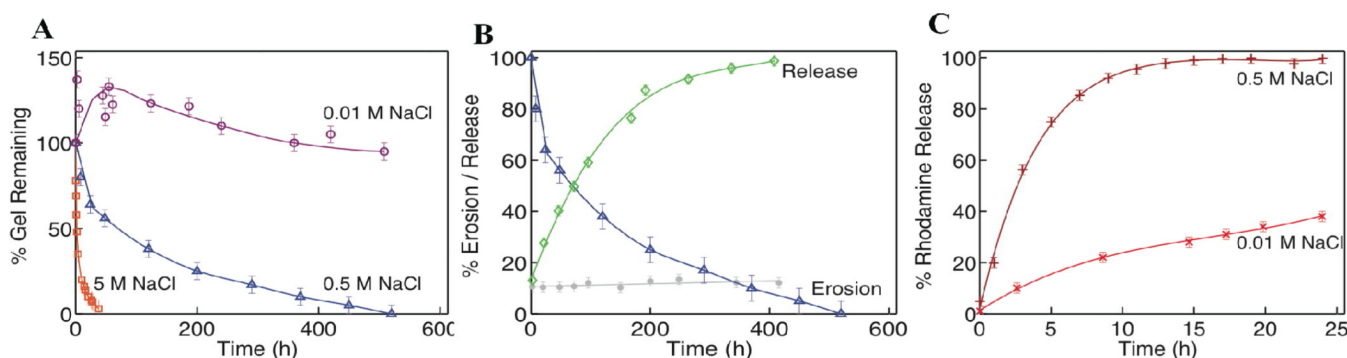
Figure 3. Erosion and content-release by TPR smart-gels
(A) A piece of gel was placed into a solution of 0.01M sodium phosphate pH 7.4, at different ionic strengths, 25 °C and removed and weighed at various times following immersion. The percent gel mass remaining is plotted versus time for the different ionic strength solutions. (B) An aliquot of fluorescent protein (mVFP) or (C) the small molecule rhodamine (MW 422 Da) was entrapped during gelation. The release of entrapped molecule was monitored as a function of time, following the increase in fluorescence of the solution in which the gel was immersed. These measurements were made in DMEM (Dulbecco/Vogt modified Eagle's minimal essential medium), a commonly used tissue culture medium, which has an ionic strength of 166 mM, pH 7.4, at 37°C. Release of the 26 kDa mVFP protein from the gel clearly mirrors gel erosion. Note that there is virtually no release in the 30 mM ionic strength solution (grey circles). (C) Data are shown for 0.01M sodium phosphate pH 7.4, plus 0.01M NaCl (light red) or plus 0.5M NaCl (dark red) at 25oC. Release of rhodamine is far more rapid than the erosion of the gel. The lines through the points in all plots are included as a guide for the eye.